Available online at www.sciencedirect.com
ScienceDirect
Applied Catalysis B: Environmental 79 (2008) 1–7
APPLIED CATALYSIS B: ENVIRONMENTAL
www.elsevier.com/locate/apcatb

Synthesis and characterization of high performance Pt-($Pr_xCe_yO_z$)/C catalysts for methanol electrooxidation

Zhicheng Tang, Gongxuan Lu *

State Key Laboratory for Oxo Synthesis and Selective Oxidation, Lanzhou Institute of Chemical Physics, Chinese Academy of Sciences and Graduate School of the Chinese Academy of Sciences, Lanzhou 730000, China

Received 7 December 2006; received in revised form 1 September 2007; accepted 24 September 2007
Available online 9 October 2007

Abstract

In this paper, $Pr_xCe_yO_z$ (x/y = 3/1, 1/1, 1/3) modified Pt/C catalysts were prepared by wet precipitation and reduction method. The catalysts were characterized by transmission electron microscopy (TEM), X-ray diffraction (XRD) and energy dispersive X-ray analysis (EDX). TEM showed that Pt nanoparticles were uniformly dispersed on the surface of carbon support with an average particle size of 4.0–5.0 nm in the Pt-($Pr_xCe_yO_z$)/C catalysts. XRD showed that all the Pt-($Pr_xCe_yO_z$)/C catalysts displayed the typical character of Pt face centered cubic (fcc) phase. XRD and EDX analysis indicated that the rare earth oxides exist in an amorphous form. The Pt-($Pr_xCe_yO_z$)/C electrocatalysts were compared with the Pt/C, Pt_3-$(PrO_x)_1$/C and Pt_3-$(CeO_x)_1$/C catalysts in terms of electrochemical activity and stability for methanol electrooxidation using cyclic voltammetry (CV) and chronoamperometry (CA) in 0.5 M H_2SO_4 + 0.5 M CH_3OH solutions. The CO-tolerance experiment was measured in the CO-saturated 0.5 M H_2SO_4 solutions. The results showed that the Pt-($Pr_1Ce_1O_z$)/C catalyst had the highest catalytic activity, the best stability and CO-tolerance, which could be used as a suitable electrocatalyst for direct methanol fuel cell.

Keywords: Methanol electrooxidation; Direct methanol fuel cell; Rare earth oxides; Electrocatalyst; Electrocatalytic reaction

1. Introduction

In the past few decades, direct methanol fuel cells (DMFCs) have attracted much attention for their potential application as clean and mobile power sources due to its advantages of low operating temperature (<100 °C), easy transportation and storage of the fuel, high energy efficiency and low exhaustion, and fast start-up [1–3]. However, the slow rate of anode methanol oxidation at low temperature and the methanol leakage from anode to cathode are the main challenges for the commercialization of DMFCs [4]. As we know, Pt is the most active electrocatalyst for methanol electrooxidation, but intermediate species of CO adsorb on the surface and inhibit the oxidation reaction [5]. Therefore, Pt-based alloy or nanocomposite catalysts by alloying or mixing platinum with other element need to be designed and synthesized. The CO-poisoned Pt can be regenerated via the reaction of surface CO with oxygen-containing species associated with an element such as ruthenium to yield CO_2 [6]. High activity, stability and CO-tolerance of Pt-based electrocatalysts under acid environment are suitable for electrooxidation of many small molecules such as methanol. So it is necessary to prepare some appropriate anode catalysts with high activity, stability and CO-tolerance for methanol electrooxidation. In order to improve the performance of methanol electrooxidation, many catalysts such as PtRu, PtSn, PtRe and PtOs have been reported [7–10]. The methods such as impregnation, colloid, micro-emulsion, polyol reduction and plasma treatment have been applied [11–15].

At present, PtRu/C electrocatalyst is widely adopted as an anode electrocatalyst in DMFCs [16–18]. However, the activity and stability of the state of art PtRu/C anode electrocatalyst cannot meet the demands for practical applications. In addition, the ruthenium element is a noble metal. Therefore, it is necessary to search for suitable electrocatalysts in place of PtRu/C catalyst for DMFCs.

In the recent years, it has been identified that the rare earth oxides exhibit a number of characteristics for catalytic reaction [19–24]. Ceria-based electrocatalysts have been reported for

* Corresponding author. Tel.: +86 931 4968178; fax: +86 931 4968178.
E-mail address: gxlu@lzb.ac.cn (G. Lu).

0926-3373/$ – see front matter © 2007 Elsevier B.V. All rights reserved.
doi:10.1016/j.apcatb.2007.09.043

methanol electrooxidation by Shen and cabrera [23,24]. In our previous work, we found rare earth oxides LnO_x (Ln = Sc, Y, La, Ce, Pr and Nd) could modify the catalyst performances for methanol electrooxidation in H_2SO_4 solution [25]. The Pt_3-$(PrO_x)_1$/C and Pt_3-$(CeO_x)_1$/C catalysts showed higher electrocatalytic activities than other LnO_x modified Pt/C electrocatalysts. In this present paper, we investigate the effect of the addition of the mixture of Pr_2O_3 and CeO_2 to Pt/C catalyst on the catalytic activity of methanol electrooxidation in H_2SO_4 solution. A series of Pt-$(Pr_xCe_yO_z)$/C electrocatalysts with different Pr/Ce ratios (Pr/Ce = 3/1, 1/1, 1/3) are prepared. The electrocatalytic performance is evaluated using cyclic voltammetry (CV), chronoamperometry (CA) and CO-stripping voltammetry. The catalysts are characterized by means of XRD, TEM and EDX analysis.

2. Experimental

2.1. Catalyst preparation

All chemicals were analytically pure and used as received. Active carbon of Vulcan XC-72 with a BET area of about 240 $m^2\ g^{-1}$ (Cabot Corp.) was used as carrier. $Ce(NO_3)_2$, Pr_2O_3 and H_2PtCl_6 were used as precursors of Ce, Pr and Pt, respectively.

Pt-$(Pr_xCe_yO_z)$/C (x/y = 3/1, 1/1, 1/3) catalysts were prepared according to the former report [25]. First, Pr_2O_3 was dissolved in concentrated HNO_3. Then the rare earth precursors were dissolved in the mixture of distilled water and ethanol (v:v = 1:1) and mixed with carbon black (Vulcan XC-72). After ultrasonically mixed, Na_2CO_3 aqueous solution was then added into the mixture to form precipitates. The precipitates were washed and dried in oven at 373 K for 10 h. The materials were finally calcinated at 600 °C for 2 h in Ar atmosphere to get $Pr_xCe_yO_z$/C (the mixture of Pr_2O_3 and CeO_2 was defined as $Pr_xCe_yO_z$/C). Pt-$(Pr_xCe_yO_z)$/C catalysts were prepared by the reduction of H_2PtCl_6 with $NaBH_4$ on $Pr_xCe_yO_z$/C powders. The nominal loading of Pt + $Pr_xCe_yO_z$ in the catalyst was 10%, and the molar ratio of Pt to $Pr_xCe_yO_z$ was 3/1. All catalysts were marked as Pt-$(Pr_xCe_yO_z)$/C, where the subscript x/y denoted the atomic ratio of Pr to Ce.

2.2. Physical characterization

The samples after reaction were transferred under N_2 atmosphere to the diffractometer, and powder X-ray diffraction (XRD) patterns of the samples were recorded on a Rigaku B/Max-RB diffractometer with a nickel filtrated Cu Kα radiation, 2θ angles from 10 to 90° were recorded at a scanning speed of 2° min^{-1}.

Specimens were prepared for TEM analysis by ultrasonically suspending the catalyst powder in ethanol. A drop of suspension was then applied onto clean copper grids and dried in air. Samples were examined using the JEOL JEM-2010 electron microscope operated at 100 kV.

The bulk composition of the as-prepared catalysts was evaluated by energy dispersive X-ray analysis (EDX) in a JEOL JSM-5600LV scanning electron microscopy (the operating voltage: 20 kV).

2.3. Preparation of electrodes and electrochemical measurements

Electrochemical activities of catalysts were measured by cyclic voltammetry (CV) and chronoamperometry (CA) methods using a standard three-electrode cell at the computer-controlled CHI660A electrochemical workstation. 5.0 mg of catalysts were suspended in 1.0 ml ethanol, and 20 μl 10.0% Nafion was added as adhesive and proton conductor. The mixtures were ultrasonically scattered for 10 min to form homogeneous ink. Then 20 μl ink was dropped on the glassy carbon (GC) electrode to act as the working electrode. A Pt wire and saturated calomel electrode (SCE) were used as the counter and reference electrode, respectively. Methanol oxidation experiment was measured in 0.5 M H_2SO_4 + 0.5 M CH_3OH solutions at room temperature. For all experiments the sweep rate was 50 mV s^{-1}. The chronoamperometric curves were investigated in a solution of 0.5 M H_2SO_4 + 0.5 M CH_3OH at 0.65 V vs. SCE at room temperature.

Before the CO-stripping measurement, the electrode was first electrochemically cleaned in 0.5 M H_2SO_4 solutions by cycling voltammetry scan between −0.25 and 1.0 V in an N_2-saturated solution. After that, CO was adsorbed onto the electrode by bubbling CO gas in the 0.5 M H_2SO_4 solutions for 10 min. Then the solution was again purged with high purity N_2 for 10 min to remove CO. Stripping voltammetry data were collected between −0.25 and 1.0 V vs. SCE with a scan rate of 50 mV s^{-1}.

3. Results and discussion

The XRD patterns of Pt-$(Pr_xCe_yO_z)$/C with different ratios of Pr/Ce, Pt_3-$(PrO_x)_1$/C, Pt_3-$(CeO_x)_1$ and Pt/C catalysts are shown in Fig. 1. The diffraction peak at 20–25° observed in all the XRD patterns of carbon-supported catalysts is due to the (0 0 2) plane of the hexagonal structure of Vulcan XC-72 carbon [26].

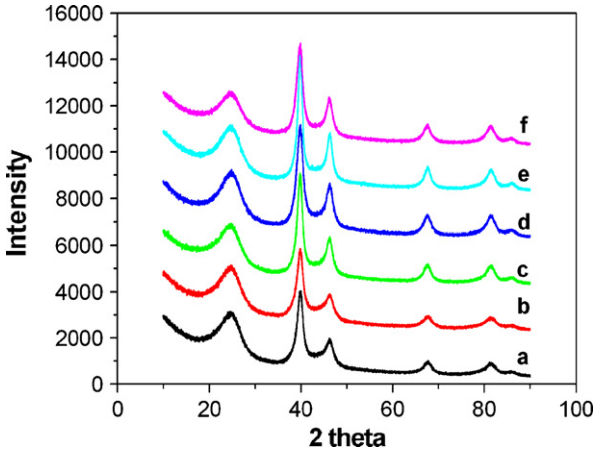

Fig. 1. X-ray diffraction patterns of Pt/C and rare earth oxides modified Pt/C electrocatalysts. (a) Pt-$(Pr_3Ce_1O_z)$/C; (b) Pt-$(Pr_1Ce_1O_z)$/C; (c) Pt-$(Pr_1Ce_3O_z)$/C; (d) Pt_3-$(PrO_x)_1$/C; (e) Pt_3-$(CeO_x)_1$/C and (f) Pt/C.

Table 1
XRD and TEM results of Pt/C and rare earth oxides modified Pt/C electrocatalysts

Catalyst	Mean particle size (nm)		Lattice parameter (Å)
	TEM	XRD	
Pt-($Pr_3Ce_1O_z$)/C	4.6	4.9	3.916
Pt-($Pr_1Ce_1O_z$)/C	4.2	4.4	3.922
Pt-($Pr_1Ce_3O_z$)/C	4.7	5.1	3.922
Pt_3-(PrO_x)$_1$/C	5.0	5.4	3.917
Pt_3-(CeO_x)$_1$/C	6.5	6.6	3.912
Pt/C	6.9	7.1	3.915

The diffraction peaks at about 39, 46, 68, 81 and 85° are due to Pt (1 1 1), (2 0 0), (2 2 0), (3 1 1) and (2 2 2) plane, respectively, which represents the typical character of Pt face centered cubic (fcc) phase [26]. There are no other distinct reflection peaks in all spectra than those of the peaks mentioned above, indicating that all those catalysts have prevailed Pt (fcc) crystal structure. No peaks of rare earth oxides suggest that rare earth oxides maybe have an amorphous structure. The (2 2 0) reflection peak of Pt is used to calculate the average particle size according to the Scherrer formula [26], which are summarized in Table 1. In our previous paper [25], the average particle size of Pt nanoparticles in the Pt/C catalyst was found to be 7.1 nm, and larger than that in the Pt_3-(CeO_x)$_1$/C and Pt_3-(PrO_x)$_1$/C catalysts. In this present paper, however, the average particle size of Pt nanoparticles in the Pt-($Pr_xCe_yO_z$)/C catalysts decreases obviously in comparison with that in the Pt_3-(CeO_x)$_1$/C and Pt_3-(PrO_x)$_1$/C catalysts, indicating that the addition of the mixture of Pr_2O_3 and CeO_2 can inhibit the agglomeration of Pt nanoparticles. Especially, the Pt nanoparticles in the Pt-($Pr_1Ce_1O_z$)/C catalyst have the smallest average particle size of 4.4 nm. The lattice parameter of Pt nanoparticles in the Pt-($Pr_3Ce_1O_z$)/C, Pt-($Pr_1Ce_1O_z$)/C and Pt-($Pr_1Ce_3O_z$)/C catalysts is estimated to be 3.916, 3.922 and 3.922 Å, respectively, which approaches that in the Pt/C, Pt_3-(CeO_x)$_1$/C and Pt_3-(PrO_x)$_1$/C catalysts. There is no shift in the diffraction peaks of Pt in the catalysts, indicating that the addition of the mixture of Pr_2O_3 and CeO_2 has no effect on the crystalline lattice of Pt. The lattice parameter obtained from the XRD patterns are listed in Table 1.

Fig. 2 shows the typical TEM images of Pt-($Pr_xCe_yO_z$)/C catalysts. In these TEM images, the semi-transparent particles are carbon black, and the black dots are the dispersed platinum. Rare earth oxides do not appear because they disperse in the amorphous form, which has been characterized by XRD. As shown in Fig. 2, the Pt nanoparticles in the Pt-($Pr_xCe_yO_z$)/C catalysts are uniform and well distributed. Based on the measurements of 200 particles in random regions, the average particle size of Pt nanoparticles is estimated to be 4.6, 4.2 and 4.7 nm for the Pt-($Pr_3Ce_1O_z$)/C, Pt-($Pr_1Ce_1O_z$)/C and Pt-($Pr_1Ce_3O_z$)/C catalysts, respectively. The average particle size of Pt nanoparticles for the Pt-($Pr_1Ce_1O_z$)/C catalyst is found to be about 4.2 nm, which is about 0.8, 2.3 and 2.7 nm lower than that for the Pt_3-(PrO_x)$_1$/C, Pt_3-(CeO_x)$_1$/C and Pt/C catalysts, respectively. The formation and dispersion of Pt nanoparticles on the carbon support may be due to the function of the mixture of Pr_2O_3 and CeO_2. The average particle size obtained from the TEM images is listed in Table 1. By examining the XRD and TEM results shown in Table 1, it can be found that the values of the average particle size obtained by TEM analysis are almost in good agreement with those calculated from the XRD results. The result of element analysis on the Pt-($Pr_1Ce_1O_z$)/C catalyst is shown in Fig. 3. The EDX analysis of the Pt-($Pr_1Ce_1O_z$)/C electrocatalyst proves the coexistence of C, Pt, Ce and Pr. The XRD and EDX analysis results show that the rare earth oxides exist in an amorphous form.

The cyclic voltammogram curves of Pt-($Pr_xCe_yO_z$)/C catalysts with different ratios of Pr/Ce in 0.5 M H_2SO_4 + 0.5 M CH_3OH solutions at a scan rate of 50 mV s^{-1} are shown in Fig. 4. The CV curves for methanol electrooxidation on the Pt/C, Pt_3-(PrO_x)$_1$/C and Pt_3-(CeO_x)$_1$/C catalysts are also presented in Fig. 4 for comparison. The peak current density, i.e., mass activity, which is defined as the ratio of peak current obtained from the forward CV scans to the mass of Pt in the electrode, is used to evaluate the activity of catalysts. As can be seen from Fig. 4, there is no significant shape difference among the voltammograms of methanol oxidation on the Pt/C, Pt_3-(PrO_x)$_1$/C, Pt_3-(CeO_x)$_1$/C and all the Pt-($Pr_xCe_yO_z$)/C catalysts. Peaks appear in both the forward and reverse scans. The positive peak potential and corresponding peak current density of methanol electrooxidation are listed in Table 2. From Fig. 4 and Table 2, it is clear that the addition of the mixture of Pr_2O_3 and CeO_2 to Pt/C shifts the peak potential of methanol electrooxidation to negative direction in comparison with the Pt_3-(PrO_x)$_1$/C and Pt_3-(CeO_x)$_1$/C electrocatalysts. The forward scan peak potential for the Pt_3-(PrO_x)$_1$/C, Pt_3-(CeO_x)$_1$/C and Pt-($Pr_xCe_yO_z$)/C electrocatalysts is about 0.71, 0.70 and 0.67 V. The negative shift of about 40 mV shows that methanol oxidation reaction are easier in the Pt-($Pr_xCe_yO_z$)/C electrocatalyst than that in the Pt_3-(PrO_x)$_1$/C and Pt_3-(CeO_x)$_1$/C electrocatalysts. The peak current density of methanol electrooxidation at the forward scan on the Pt-($Pr_xCe_yO_z$)/C catalysts follows this order: Pt-($Pr_1Ce_1O_z$)/C > Pt-($Pr_3Ce_1O_z$)/C > Pt-($Pr_1Ce_3O_z$)/C, and is far larger than that on the Pt/C and Pt_3-(CeO_x)$_1$/C catalysts. In all the Pt-($Pr_xCe_yO_z$)/C catalysts, the Pt-($Pr_1Ce_3O_z$)/C catalyst shows the lowest peak current density with a value of 90.3 mA mg^{-1}. In all the Pt-($Pr_xCe_yO_z$)/C catalysts, except that the catalytic activity of the Pt-($Pr_1Ce_3O_z$)/C catalyst approaches that of the Pt_3-(PrO_x)$_1$/C catalyst, the two others are larger than that of the Pt_3-(PrO_x)$_1$/C catalyst. The catalytic activity of all the Pt-($Pr_xCe_yO_z$)/C catalysts approaches and is even superior to that of the Pt_3-(PrO_x)$_1$/C catalyst, indicating that the addition of the mixture of Pr_2O_3 and CeO_2 favors for the methanol electrooxidation. As can be seen from Fig. 4 and Table 2, it is clear that the Pt-($Pr_1Ce_1O_z$)/C catalyst presents the highest positive peak current density and corresponding highest activity to methanol electrooxidation from the point of current density. The Pt-($Pr_1Ce_1O_z$)/C catalyst shows the highest peak current density of 118.3 mA mg^{-1} among all the catalysts and has a comparatively negative potential (0.68 V) than others, indicating that the Pt-($Pr_1Ce_1O_z$)/C catalyst is a good electrocatalyst for methanol electrooxidation.

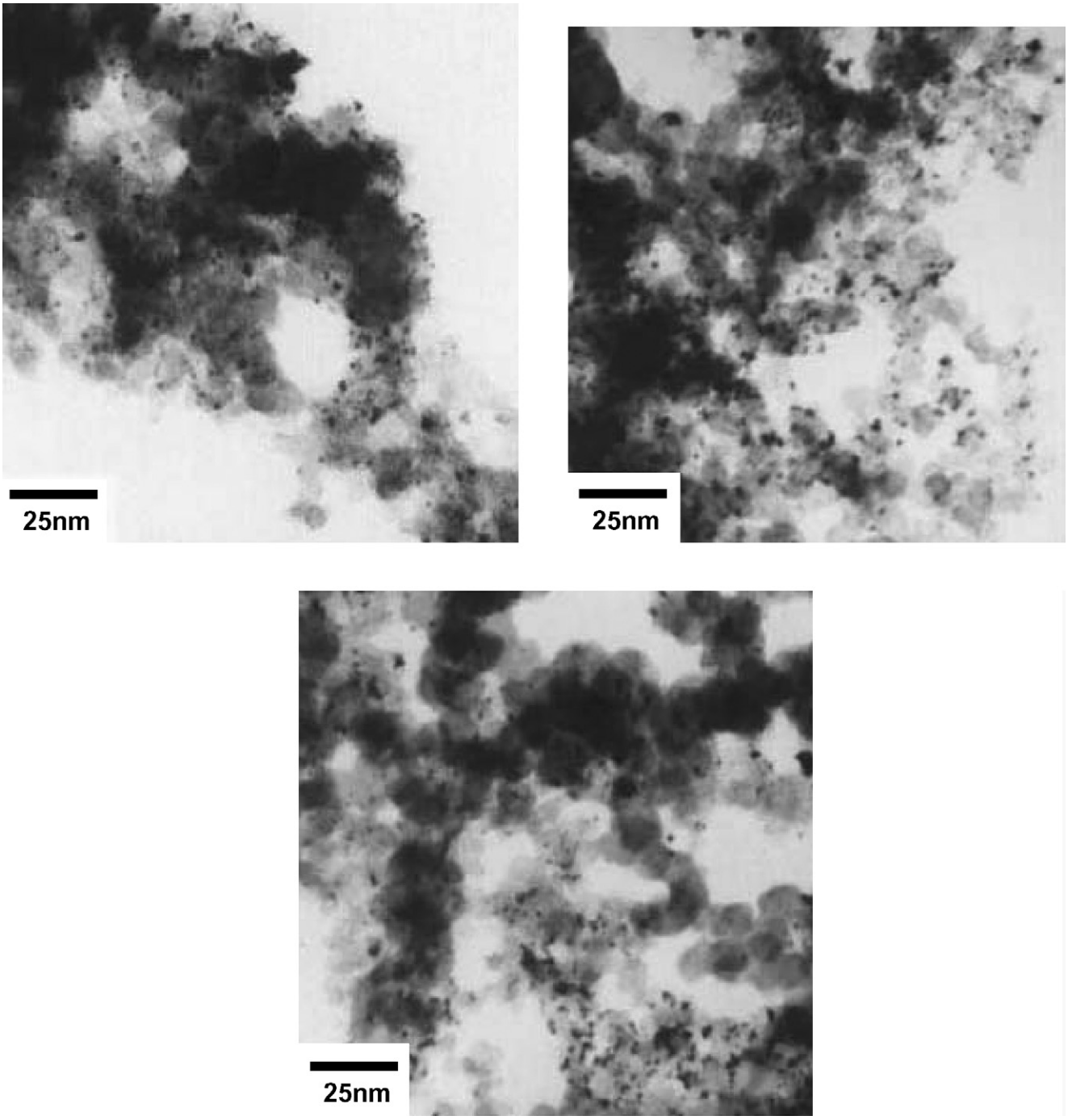

Fig. 2. TEM images of the Pt-($Pr_xCe_yO_z$)/C catalysts. (a) Pt-($Pr_3Ce_1O_z$)/C; (b) Pt-($Pr_1Ce_1O_z$)/C and (c) Pt-($Pr_1Ce_3O_z$)/C.

To measure the electrochemical stability of Pt-($Pr_xCe_yO_z$)/C catalysts for methanol electrooxidation, chronoamperometry (CA) experiments are carried out. Fig. 5 presents the typical CA curves obtained in 0.5 M H_2SO_4 + 0.5 M CH_3OH solutions at an anodic potential of 0.65 V vs. SCE. This potential is chosen because it is close to the positive peak potential of methanol electrooxidation in the cyclic voltammogram curves. In all the CA curves, there is a sharp initial current drop in the first 300 s, and follows by a slower decay. The current decay is due to that the intermediate products of methanol oxidation such as CO_{ads} and other CHO_{ads} in the electrolyte easily adsorb onto the surface of Pt nanoparticles and inhibit methanol electrooxidation. The final current density values at the end of 1000 s during chronoamperometric experiments are presented in Fig. 6. In longer runs it is found that the current density obtained on the Pt-($Pr_1Ce_1O_z$)/C catalyst is the highest. The final current density after holding the cell potential at 0.65 V vs. SCE for 1000 s decreases in this order: Pt-($Pr_1Ce_1O_z$)/C > Pt-($Pr_1Ce_3O_z$)/C ≈ Pt_3-(PrO_x)$_1$/C > Pt_3-(CeO_x)$_1$/C > Pt-($Pr_3Ce_1O_z$)/C > Pt/C. This result is nearly consistent with the CV result. The Pt-($Pr_3Ce_1O_z$)/C electrocatalyst shows a higher catalytic activity than the Pt-($Pr_1Ce_3O_z$)/C, Pt_3-(PrO_x)$_1$/C and

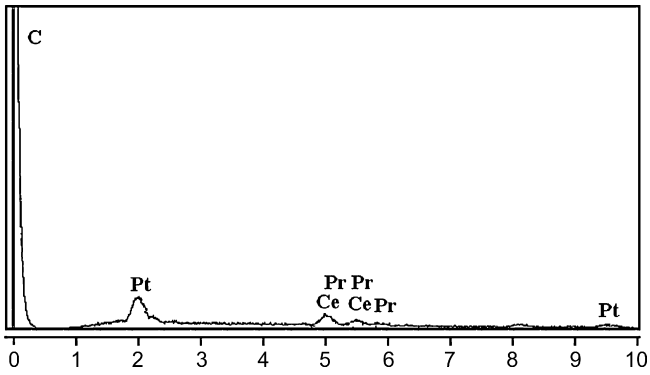

Fig. 3. EDX spectrum of the Pt-($Pr_1Ce_1O_z$)/C catalyst.

Table 2
CV results of Pt/C and rare earth oxides modified Pt/C electrocatalysts for methanol and CO electrooxidation

Catalysts	Positive peak potential (V vs. SCE)	Peak current density (mA mg^{-1})	CO peak potential (V vs. SCE)
Pt-($Pr_3Ce_1O_z$)/C	0.67	108.9	0.58
Pt-($Pr_1Ce_1O_z$)/C	0.68	118.3	0.58
Pt-($Pr_1Ce_3O_z$)/C	0.68	90.9	0.61
Pt_3-(PrO_x)$_1$/C	0.71	92.2	0.63
Pt_3-(CeO_x)1/C	0.70	56.3	0.65
Pt/C	0.66	49.1	0.66

Pt_3-(CeO_x)$_1$/C electrocatalysts, but has a worse stability than the latter. The Pt-($Pr_1Ce_1O_z$)/C electrocatalyst has the highest final current density (5.1 mA mg^{-1}) among all catalysts, which is far larger than the Pt/C electrocatalyst (1.56 mA mg^{-1}). The test shows that the Pt-($Pr_1Ce_1O_z$)/C electrocatalyst has the best electrocatalytic stability among the Pt/C, Pt_3-(CeO_x)$_1$/C, Pt_3-(PrO_x)$_1$/C and Pt-($Pr_xCe_yO_z$)/C electrocatalysts. As can be seen from the characterization of activity and stability, the Pt-($Pr_1Ce_1O_z$)/C electrocatalyst has excellent electrocatalytic activity and good stability toward methanol electrooxidation, indicating that the Pt-($Pr_1Ce_1O_z$)/C catalyst is a promising electrocatalyst for methanol electrooxidation.

CO-stripping voltammetry is an effective way to test CO-tolerance of a catalyst for the electrocatalytic oxidation of adsorbed CO on the surface of catalyst. Fig. 7 shows the typical CO-stripping voltammograms for the Pt-($Pr_3Ce_1O_z$)/C, Pt-($Pr_1Ce_1O_z$)/C, Pt-($Pr_1Ce_3O_z$)/C, Pt_3-(PrO_x)$_1$/C, Pt_3-(CeO_x)$_1$/C and Pt/C catalysts in 0.5 M H_2SO_4 solutions after complete adsorption of CO and subsequent purging of the solution with high-purity nitrogen. As can be seen from Fig. 7, the hydrogen adsorption peak appears obviously, indicating that the adsorbed CO has been oxidized completely in the first scan. No CO oxidation is monitored during the second scan for all catalysts. For comparison, the current density is evaluated using mass activity. The Pt-($Pr_1Ce_1O_z$)/C and Pt-($Pr_3Ce_1O_z$)/C catalysts have a similar CO oxidation peak potential of 0.58 V, which is about 50, 70 and 80 mV lower than the Pt_3-(PrO_x)$_1$/C, Pt_3-(CeO_x)$_1$/C and Pt/C catalysts, respectively. For the Pt-($Pr_1Ce_3O_z$)/C catalyst, the peak potential of CO oxidation is 0.61 V, which is higher than that of the Pt-($Pr_1Ce_1O_z$)/C and Pt-($Pr_3Ce_1O_z$)/C catalysts, but lower than that of the Pt_3-(PrO_x)$_1$/C, Pt_3-(CeO_x)$_1$/C and Pt/C catalysts. The peak potential of CO oxidation on the Pt_3-(PrO_x)$_1$/C and Pt_3-(CeO_x)$_1$/C catalysts is also lower than that on the Pt/C catalyst, indicating that the addition of rare earth oxides helps CO oxidation. It is interesting to note that differing from other catalysts, a ''shoulder'' peak at about 0.57 V appears on the Pt_3-(CeO_x)$_1$/C catalyst, which is similar to the report in the literature [27]. All the Pt-($Pr_xCe_yO_z$)/C electrocatalysts have a similar onset potential, which is slightly lower than the Pt_3-(PrO_x)$_1$/C, Pt_3-(CeO_x)$_1$/C and Pt/C catalysts. The overall results shows that the addition of the mixture of Pr_2O_3 and CeO_2 to Pt/C is helpful for enhancing the catalytic activity of methanol and CO electrooxidation.

Cyclic voltammograms, chronoamperometry and CO-stripping voltammograms show that the addition of the mixture of Pr_2O_3 and CeO_2 can obviously enhance the catalytic perfor-

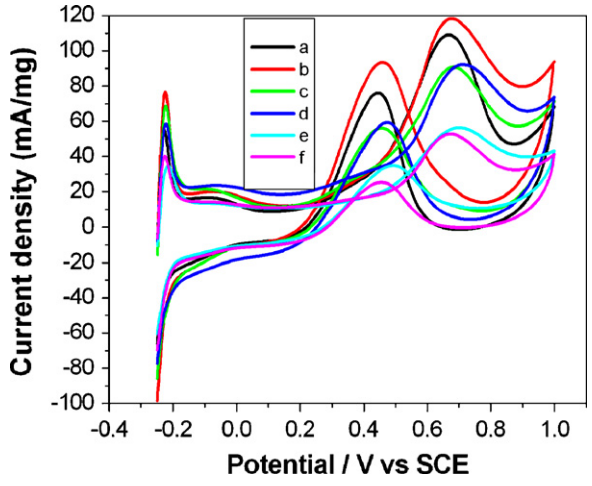

Fig. 4. Cyclic voltammograms of Pt/C and rare earth oxides modified Pt/C electrocatalysts in the 0.5 M H_2SO_4 + 0.5 M CH_3OH solutions at a sweep rate of 50 mV s^{-1}. (a) Pt-($Pr_3Ce_1O_z$)/C; (b) Pt-($Pr_1Ce_1O_z$)/C; (c) Pt-($Pr_1Ce_3O_z$)/C; (d) Pt_3-(PrO_x)$_1$/C; (e) Pt_3-(CeO_x)$_1$/C and (f) Pt/C.

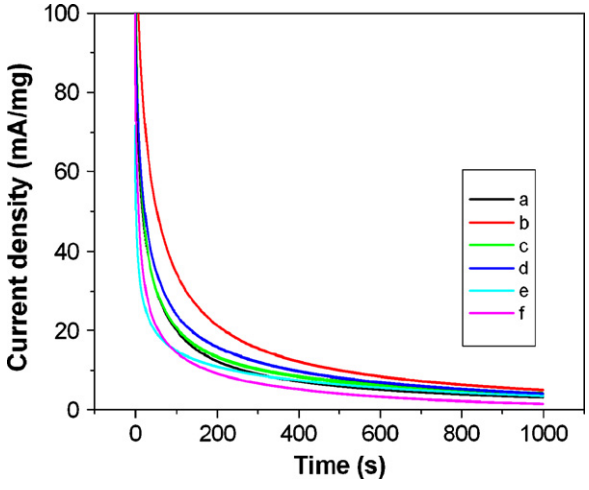

Fig. 5. Chronoamperometry of Pt/C and rare earth oxides modified Pt/C electrocatalysts in the 0.5 M H_2SO_4 + 0.5 M CH_3OH solutions at 0.65 V vs. SCE. (a) Pt-($Pr_3Ce_1O_z$)/C; (b) Pt-($Pr_1Ce_1O_z$)/C; (c) Pt-($Pr_1Ce_3O_z$)/C; (d) Pt_3-(PrO_x)$_1$/C; (e) Pt_3-(CeO_x)$_1$/C and (f) Pt/C.

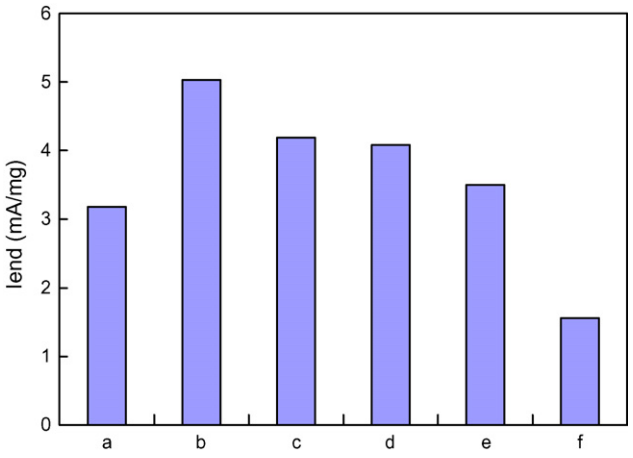

Fig. 6. Current density values at 1000 s during chronoamperometry experiments for Pt/C and rare earth oxides modified Pt/C electrocatalysts. (a) Pt-($Pr_3Ce_1O_z$)/C; (b) Pt-($Pr_1Ce_1O_z$)/C; (c) Pt-($Pr_1Ce_3O_z$)/C; (d) Pt_3-(PrO_x)$_1$/C; (e) Pt_3-(CeO_x)$_1$/C and (f) Pt/C.

mance for methanol oxidation in comparison with the individual addition of Pr_2O_3 or CeO_2. Especially, the Pt-($Pr_1Ce_1O_z$)/C catalyst has excellent electrocatalytic activity and good stability toward the methanol electrooxidation.

As we all know, rare earth oxides have been widely investigated as structural and electronic promoters to improve the activity, selectivity and thermal stability of catalysts. The most significant rare earth oxide in industrial catalysis is certainly CeO_2. The success of ceria is mainly due to the unique combination of an elevated oxygen transport capacity coupled with the ability to shift easily between reduced and oxidized state (Ce^{3+}/Ce^{4+}). However, the major drawback of pure ceria is related to thermal resistance and low-temperature activity [28]. Thermal expansion due to the reduction of Ce^{4+} to Ce^{3+} occurs at a significant rate on ceria only above 900 K but starts at room temperature when ceria is doped with praseodymium [29]. At room temperature, the mixture cerium-praseodymium oxide presents a structure in which oxygen atoms are able to migrate rapidly in the bulk. On the contrary, for ceria, high temperature must be reached to observe the behavior. This can be assigned to a significant formation of oxygen vacancies in the cerium-praseodymium oxide at room temperature. Cerium-praseodymium oxide possesses pre-existing oxygen vacancies in great number at room temperature [29,30]. Praseodymium oxide incorporated in ceria ensures the obtained material with high oxygen mobility within a large range of temperature. Oxygen vacancies and high oxygen mobility can supply sufficient surface oxygen-containing species to activate and oxidize the chemisorbed CO_{ads} intermediate species formed on the platinum surface during the methanol electrooxidation. Therefore, the addition of the mixture of Pr_2O_3 and CeO_2 is more helpful for methanol electrooxidation than individual Pr_2O_3 or CeO_2. The performance of Pt-($Pr_1Ce_1O_z$)/C is superior to that of Pt-($Pr_3Ce_1O_z$)/C and Pt-($Pr_1Ce_3O_z$)/C, which maybe attribute to the high dispersion between Pt nanoparticles and the mixture of Pr_2O_3 and CeO_2.

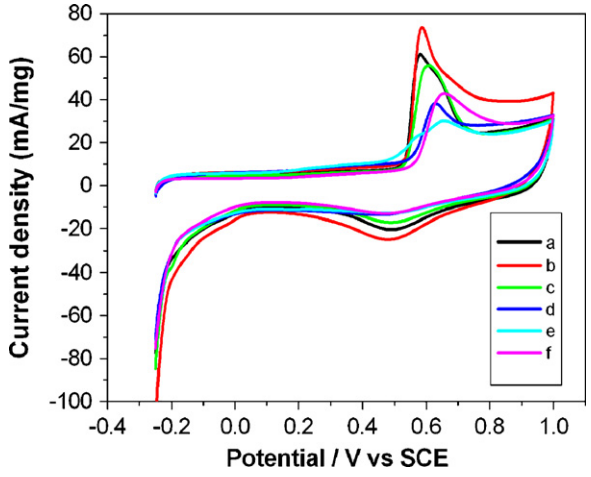

Fig. 7. CO-stripping cyclic voltammograms of Pt/C and rare earth oxides modified Pt/C electrocatalysts in the CO-saturated 0.5 M H_2SO_4 solutions at a sweep rate of 50 mV s^{-1}. (a) Pt-($Pr_3Ce_1O_z$)/C; (b) Pt-($Pr_1Ce_1O_z$)/C; (c) Pt-($Pr_1Ce_3O_z$)/C; (d) Pt_3-(PrO_x)$_1$/C; (e) Pt_3-(CeO_x)$_1$/C and (f) Pt/C.

4. Conclusion

$Pr_xCe_yO_z$ promoted Pt/C electrocatalysts were prepared by wet precipitation and reduction method. The preliminary CV results indicated that the addition of the mixture of Pr_2O_3 and CeO_2 into Pt/C catalysts could significantly improve the electrode performance for methanol electrooxidation compared to the Pt_3-(PrO_x)$_1$/C, Pt_3-(CeO_x)$_1$/C and Pt/C electrocatalysts. For the Pt-($Pr_xCe_yO_z$)/C electrocatalysts, the Pr/Ce ratios had an important effect on the catalytic activity of catalysts. The total CV, CA and CO-stripping voltammogram results showed that the Pt-($Pr_1Ce_1O_z$)/C electrocatalyst had the highest activity, the best stability and CO-tolerance than others. The better performance could attribute to sufficient surface oxygen-containing species and high oxygen mobility in the surface of the mixture of Pr_2O_3 and CeO_2.

References

[1] C. Lamy, A. Lima, V. LeRhun, F. Delime, C. Coutanceau, J.M. Léger, J. Power Sources 105 (2002) 283–296.
[2] T. Iwasita, Electrochim. Acta 47 (2002) 3663–3674.
[3] A. Hamnett, Catal. Today 38 (1997) 445–457.
[4] S. Song, W. Zhou, Z. Liang, R. Cai, G. Sun, Q. Xin, V. Stergiopoulos, P. Tsiakaras, Appl. Catal. B: Environ. 55 (2005) 65–72.
[5] M.B. de Oliveira, L.P.R. Profeti, P. Olivi, Electrochem. Commun. 7 (2005) 703–709.
[6] Q. Lu, B. Yang, L. Zhuang, J. Lu, J. Phys. Chem. B 109 (2005) 1715–1722.
[7] J. Guo, G. Sun, Q. Wang, G. Wang, Z. Zhou, S. Tang, L. Jiang, B. Zhou, Q. Xin, Carbon 44 (2006) 152–157.
[8] L. Jiang, G. Sun, S. Sun, J. Liu, S. Tang, H. Li, B. Zhou, Q. Xin, Electrochim. Acta 50 (2005) 5384–5389.
[9] K.B. Kokoh, F. Hahn, E.M. Belgsir, C. Lamy, A.R. de Andrade, P. Olivi, A.J. Motheo, G. Tremiliosi-Filho, Electrochim. Acta 49 (2004) 2077–2083.
[10] B.N. Grgur, N.M. Markovic, P.N. Ross, Electrochim. Acta 43 (1998) 3631–3635.
[11] F. Colmati, E. Antolini, E.R. Gonzalez, Appl. Catal. B: Environ. 73 (2007) 106–115.
[12] Z. Tang, D. Geng, G. Lu, J. Colloids Interf. Sci. 287 (2005) 159–166.

[13] M.V. Martínez-Huerta, S. Rojas, J.L. Gómez de la Fuente, P. Terreros, M.A. Peña, J.L.G. Fierro, Appl. Catal. B: Environ. 69 (2006) 75–84.
[14] W. Zhou, Z. Zhou, S. Song, W. Li, G. Sun, P. Tsiakaras, Q. Xin, Appl. Catal. B: Environ. 46 (2003) 273–285.
[15] Z. Tang, Q. Li, G. Lu, Carbon 45 (2007) 41–46.
[16] U.A. Paulus, U. Endruschat, G.J. Feldmeyer, T.J. Schmidt, H. Bönnemann, R.J. Behm, J. Catal. 195 (2000) 383–393.
[17] T. Kawaguchi, W. Sugimoto, Y. Murakami, Y. Takasu, J. Catal. 229 (2005) 176–184.
[18] Z. Liu, J.Y. Lee, W. Chen, M. Han, L.M. Gan, Langmuir 20 (2004) 181–187.
[19] H.M. Villullas, F.I. Mattos-Costa, L.O.S. Bulhoes, J. Phys. Chem. B 108 (2004) 12898–12903.
[20] J. Shim, C. Lee, H. Lee, J. Lee, E.J. Cairns, J. Power Sources 102 (2001) 172–177.
[21] Y. Bai, J. Wu, J. Xi, J. Wang, W. Zhu, L. Chen, X. Qiu, Electrochem. Commun. 7 (2005) 1087–1090.
[22] C. Xu, P.K. Shen, X. Ji, R. Zeng, Y. Liu, Electrochem. Commun. 7 (2005) 1305–1308.
[23] C. Xu, P.K. Shen, Chem. Commun. 19 (2004) 2238–2239.
[24] C.L. Campos, C. Roldan, M. Aponte, Y. Ishikawa, C.R. Cabrera, J. Electroanal. Chem. 581 (2005) 206–215.
[25] Z. Tang, G. Lu, J. Power Sources 162 (2006) 1067–1072.
[26] Z.B. Wang, G.P. Yin, J. Zhang, Y.C. Sun, P.F. Shi, J. Power Sources 160 (2006) 37–43.
[27] Y. Bai, J. Wu, X. Qiu, J. Xi, J. Wang, J. Li, W. Zhu, L. Chen, Appl. Catal. B: Environ. 73 (2006) 144–149.
[28] S.J. Schmieg, D.N. Belton, Appl. Catal. B: Environ. 6 (1995) 127–144.
[29] S. Rossignol, F. Gérard, D. Mesnard, C. Kappenstein, D. Duprez, J. Mater. Chem. 13 (2003) 3017–3020.
[30] S. Rossignol, C. Descorme, C. Kappenstein, D. Duprez, J. Mater. Chem. 11 (2001) 2587–2592.